Local Heterogeneity in the Pressure Denaturation of the Coiled-Coil Tropomyosin Because of Subdomain Folding Units†

Marisa C. Suarez,‡ Sherwin S. Lehrer,§ and Jerson L. Silva*,‡,||

Programa de Biologia Estrutural, Departamento de Bioquímica Médica, Instituto de Ciências Biomédicas, and Centro Nacional de Ressonância Magnética Nuclear de Macromoléculas, Universidade Federal do Rio de Janeiro, 21941-590 Rio de Janeiro, Brazil, and Muscle and Motility Group, Boston Biomedical Research Institute, Watertown, Massachusetts 02472-2829

Received September 6, 2000; Revised Manuscript Received November 28, 2000

ABSTRACT: Coiled-coil domains mediate the oligomerization of many proteins. The assembly of long coiled coils, such as tropomyosin, presupposes the existence of intermediates. These intermediates are not well-known for tropomyosin. Hydrostatic pressure affects the equilibrium between denatured and native forms in the direction of the form that occupies a smaller volume. The hydrophobic core is the region more sensitive to pressure, which leads in most cases to the population of intermediates. Here, we used *N*-(1-pyrenyl)iodoacetamide covalently bound to cysteine residues of tropomyosin (PIATm) and high hydrostatic pressure to assess the chain interaction and the inherent instability of the coiled-coil molecule. The native and denatured states of tropomyosin were determined from the pyrene excimer fluorescence. The combination of low temperature and high pressure permitted the attainment of the full denaturation of tropomyosin without the separation of the subunits. High-temperature denaturation of Tm leads to a great exchange between labeled and unlabeled Tm subunits, indicating subunit dissociation linked to unfolding. In contrast, under high pressure, unlabeled and labeled tropomyosin molecules do not exchange, demonstrating that the denatured species are dimeric. The decrease of the concentration dependence of PIATm corroborates the idea that pressure produces subdomain denaturation and that the polypeptide chains do not separate. Substantial unfolding of tropomyosin was also verified by measurements of tyrosine fluorescence and bis-ANS binding. Our results indicate the presence of independent folding subdomains with different susceptibilities to pressure along the length of the coiled-coil structure of tropomyosin.

Coiled-coil sequences in proteins consist of heptad repeats containing two characteristic nonpolar positions (*1*). The coiled-coil motif is found in many proteins, including tropomyosin (Tm), myosin, keratin, basic-region leucine zippers, and membrane-fusion proteins from several viruses (*1*−*6*). The coiled-coil structure consists of two right-handed α helices wrapped around one another with a slight left-handed superhelical twist. The signature of a coiled-coil structure is the unique packing of amino acid side chains in the core of the bundle, called knobs-into-holes, in which a residue (knob) from one helix packs into a space surrounded by four side chains (hole) of the facing helix (*1*).

Coiled-coil proteins have a characteristic seven-residue repeat, $(abcdefg)_n$, with nonpolar residues at positions a and d and polar residues in other positions. The coiled-coil motif has been widely used as a model to study protein folding (*7*−*10*). Although small coiled coils seem to dissociate and unfold cooperatively, the unfolding of larger coiled coils such as Tm is more complicated and seems to involve intermediates. At neutral pH, the thermal unfolding of Tm occurs with a pretransition, where 20% ellipticity is lost, followed by complete cooperative unfolding at higher temperatures (*11*). The pretransition has been ascribed to local unfolding (*12*), loss of the coiled coil but not helical structure (*13*), and noncooperative melting of the helix (*14*). Lowering the pH, a commonly used way to investigate intermediates, makes the Tm dimer highly stable to thermal denaturation (*15*). Lumb and co-workers (*8*) tackled the possibility of the existence of subdomain folding in a coiled coil using the leucine zipper peptide of the yeast bZIP transcription factor GCN4. They found that cooperatively folded subdomains are the important determinants of the folding of the coiled coil (*8*).

Tm is one of the components of the muscle thin-filament system involved in the Ca^{2+} control of striated muscle contraction. It is a coiled coil of two parallel α-helical polypeptide chains that are stabilized by large hydrophobic interactions between nonpolar side chains and electrostatic interactions between charged side chains (*16*). Rabbit skeletal Tm contains two chains, α and *β*, which differ slightly in amino acid sequence. The α chain contains a single cysteine at position 190, whereas the *β* chain contains two cysteines at positions 190 and 36 (*17*). A previous study revealed that

† This work was supported in part by an International Grant from the Howard Hughes Medical Institute to J.L.S.; by grants from Conselho Nacional de Desenvolvimento Científico e Tecnológico (CNPq—PRONEX Program), Fundação de Apoio a Pesquisa do Estado do Rio de Janeiro Carlos Chagas Filho (FAPERJ), and Financiadora de Estudos e Projetos (FINEP) of Brazil to J.L.S; and by a National Institutes of Health Grant (NIH HL22461) to S.S.L. M.C.S. has a graduate fellowship from CAPES.

* To whom correspondence should be addressed. E-mail: jerson@bioqmed.ufrj.br. Phone: (5521) 590-4548. Fax: (5521) 270-8647.

‡ Universidade Federal do Rio de Janeiro.

§ Boston Biomedical Research Institute.

|| J.L.S. is a Howard Hughes Medical Institute International Scholar.

10.1021/bi0020978 CCC: $20.00
Published on Web 01/09/2001

troponin T interacts with Tm to anchor the troponin complex to the thin filament in two regions, one near the cysteines 190 and one along the carboxyl-terminal area of Tm (*18*).

Here, we use *N*-(1-pyrenyl)iodoacetamide covalently bound to both cysteines (Cys 190) of the two chains of Tm (PIATm) to follow the conformational changes of the protein. In the dimer, these two residues are in close proximity. This region appears to be one of the more unstable sites in the molecule, and it may have an important function in the regulation of myosin−actin interaction. We use high hydrostatic pressure to evaluate chain interaction and the inherent instability of the molecule in the region of Cys 190 (*11*). The *N*-(1-pyrenyl)iodoacetamide (PIA) has only a small effect on the stability of the protein and reveals information about the conformational changes of Tm by fluorescence (*19*).

Hydrostatic pressure has been used to induce denaturation and subunit dissociation of proteins (*20*−*25*) and macromolecular assemblages (*26*−*30*). Pressures in the range of 1−3 kbar provide important information on protein folding intermediates (*28*). In addition, pressure studies can be used to determine thermodynamic parameters such as the volume change (ΔV) and the Gibbs free energy (ΔG) upon folding or association of proteins at atmospheric pressure (*20*, *22*). Moreover, at 2.4 kbar, the freezing point of water decreases to −20 °C. Because hydrophobic interactions are weakened by the decrease in temperature and there are extensive interactions between chains in PIATm, we subject PIATm to high pressure and low temperature to characterize the effects of these two types of perturbations on the coiled-coil structure. Our results indicate the presence of independent folding subdomains with different susceptibilities to pressure along the length of the Tm coiled coil.

MATERIAL AND METHODS

Chemicals. All reagents were of analytical grade. Bis-ANS was obtained from Molecular Probes (Eugene, OR). Rabbit skeletal Tm was prepared and labeled with PIA, as described previously (*19*). PIATm concentration was determined by the BCA-protein assay (Pierce), using unlabeled Tm as a standard, and the PIA concentration bound to Tm was determined by using $\epsilon_{344} = 2.2 \times 10^4$. The labeling ratio of pyrene to Tm was 2. The PIATm was lyophilized and resuspended in 50 mM Tris-HCl, pH 7.5, and 500 mM NaCl. The PIATm concentration was confirmed spectrophotometrically using the same extinction coefficient. All of the experiments were performed in the standard buffer (50 mM Tris-HCl (pH 7.5) in 500 mM NaCl). Tris-HCl was selected because the dependence of its pK_a on pressure is small. At 3 kbar, the value of the pK_a increases by only 0.1 unit (*31*).

Fluorescence Studies under Pressure. The high-pressure bomb has been described by Paladini and Weber (*32*). All data were recorded on an ISS200 or ISSK2 spectrofluorometer purchased from ISS (Champaign, IL). PIATm emission spectra were obtained by setting the excitation at 342 nm and measuring the emission from 370 to 570 nm. The tyrosine spectra were attained by exciting the sample at 278 nm and collecting the emission from 295 to 400 nm. Bis-ANS spectra were obtained by setting the excitation at 360 nm and measuring the emission from 400 to 600 nm.

The tyrosine fluorescence center of spectral mass at pressure p (νp) was calculated from the spectra by

$$\langle \nu p \rangle = \sum \nu i \times Fi / \sum Fi \quad (1)$$

where Fi is the fluorescence emitted at wavenumber νi.

The pyrene excimer ratio (I_{485}/I_{385}), the center of the spectral mass of tyrosine, and the spectral area of bis-ANS were converted into the extent of reaction according to

$$\alpha_p = (R_p - R_i)/(R_f - R_i) \quad (2)$$

where R_p is the value at each pressure, R_i is the value at 1.0 bar, and R_f is the value at 2.4 kbar.

RESULTS

Effects of Pressure on PIATm. The fluorescence spectrum of PIATm is composed of two main peaks, one at 385 nm with a shoulder at 405 nm, corresponding to the emission of monomeric dye (noncomplexed excited pyrene), and a second peak at 485 nm, which is related to the formation of a dimer of pyrenes and arises from the proximity of the two adjacent cysteines (one in each chain; Figure 1). The excited-state pyrene of one subunit interacts with the ground-state pyrene in the adjacent subunit to form the excimer dimer (*19*).

Previous studies in which Tm labeled at Cys 190 using pyrenylmaleimide (PMTm) was denatured by guanidine hydrochloride showed a decrease of excimer fluorescence and a loss in the ellipticity at 222 nm. An initial decrease in excimer fluorescence preceded protein unfolding, suggesting a region of instability in the molecule near Cys 190 (*33*). However, most of the decrease in the excimer fluorescence was correlated with chain dissociation and denaturation. The same decrease in excimer fluorescence was observed when PMTm and PIATm were subjected to temperatures higher than 33 and 44 °C, respectively (*19*, *34*). These results indicated that emission at 485 nm was dependent on the integrity of the coiled-coil dimer and that an increase or a decrease in the fluorescence intensity at 485 nm could be used to infer the degree of association/folding of Tm.

The effect of pressure on PIATm based on the fluorescence intensity ratio (I_{485}/I_{385}) is shown in Figure 2. Although a plateau is not reached, the decrease in excimer fluorescence with an increase in pressure from 1 bar to 2.4 kbar is about 70% of that promoted by the thermal unfolding of Tm. After the return to atmospheric pressure (open circle), the fluorescence intensity ratio recovered ∼85% of the value observed for the nonpressurized sample. The residual excimer formation under pressure can be explained either by incomplete dissociation (∼70%) or by the denaturation of Tm without separation of the chains. Because the dissociation of a dimeric protein is a concentration-dependent process, different concentrations of PIATm were subjected to increasing pressure. For a stochastic equilibrium between dimer and monomer, a displacement of the pressure dissociation curve with a change in protein concentration is expected (*32*, *35*−*37*). Figure 3 shows the pressure-induced changes in the I_{485}/I_{385} ratio expressed as the degree of denaturation (α; eq 2) for two concentrations of PIATm (21 and 210 μg/mL). The pressure necessary to promote half-denaturation ($p_{1/2}$) shifted to higher pressure ($\Delta p_{1/2} = 200$ bar) when the PIATm concentration was increased 10-fold. The standard volume change of dissociation (ΔV) and the dissociation constant at atmospheric pressure (K_{atm}) can be calculated from the

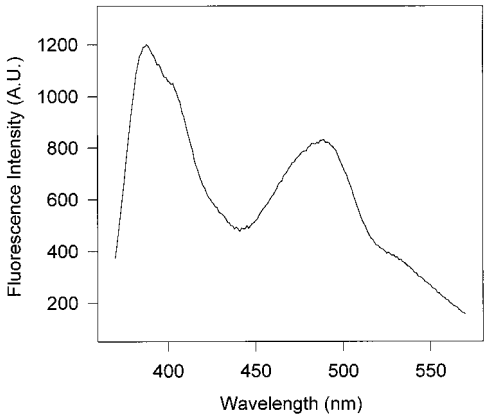

FIGURE 1: Fluorescence emission spectra of PIATm (49 μg/mL) at atmospheric pressure and 25 °C. Excitation wavelength was 342 nm, and the emission was collected from 370 to 570 nm. The solvent conditions were 50 mM Tris-HCl, pH 7.5, and 500 mM NaCl.

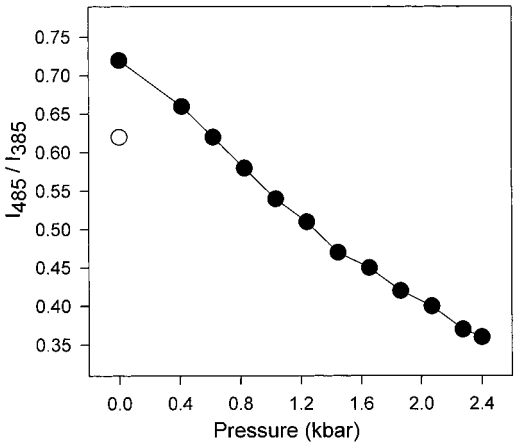

FIGURE 2: Effect of pressure on the PIATm fluorescence intensity ratio (I_{485}/I_{385}). PIATm was subjected to increasing pressure steps of 200 bar, at 25 °C (●). The open symbol represents the fluorescence intensity ratio of PIATm after the return to atmospheric pressure. The values of α_p were determined according to eq 2 and by considering the end point R_f, the intensity ratio produced by urea denaturation. The concentration of PIATm was 49 μg/mL. Other conditions were the same as those in Figure 1.

thermodynamic relation (*20*)

$$\ln[\alpha_p{}^n/(1-\alpha_p)] = p(\Delta V/RT) + \ln[K_{atm}/n^n C^{n-1}] \quad (3)$$

where n is the number of subunits and C is the protein concentration, at a series of different pressures.

If a dimer−monomer dissociation process is assumed ($n = 2$), the volume change determined from the pressure curves is −57 mL/mol (inset, Figure 3). This volume change is in the same range as that found for the dissociation or denaturation of other proteins (−40 to −150 mL/mol). However, the theoretical value of Δp (calculated from eq 4 below) for $C_2/C_1 = 10$ is 609 bar, well above the value of Δp obtained experimentally (200 bar).

$$\Delta p = (n-1)(RT/\Delta V)\ln(C_2/C_1) \quad (4)$$

This dramatic decrease of dependence on protein concentration is not common for the pressure dissociation of dimeric proteins (*20*, *28*). This decrease in concentration dependence can be explained by two hypotheses: (1) There is heterogeneity in the population of Tm molecules, as has been observed for large multimeric complexes (*38*−*41*) or (2) pressure promotes subdomain denaturation, and the polypeptide chains do not separate. In the latter hypothesis, the heterogeneity is along the coiled-coil structure of Tm. In other words, the PIATm subunits are not rigid rods with a homogeneous distribution of intramolecular forces, but rather they constitute an inhomogeneous molecular zipper. Therefore, although substantial denaturation occurs, there are coiled-coil segments that are resistant to pressure. The values of ΔV for $n = 1$ (local denaturation) and $n = 2$ (dissociation/denaturation) were −34 and −57 mL/mol, respectively.

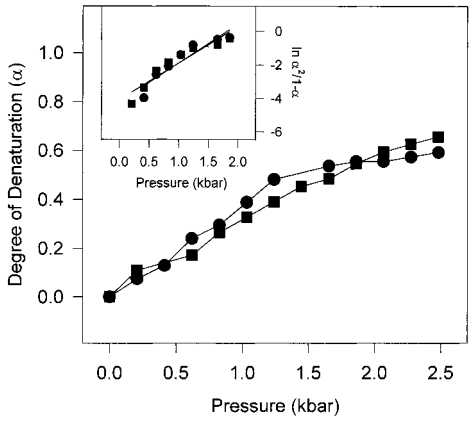

FIGURE 3: Effect of protein concentrations on the pressure denaturation of PIATm. Plot of the degree of denaturation as a function of pressure. The PIATm concentrations were 21 (●) and 210 μg/mL (■). Inset: plot of $\ln[\alpha_p{}^n/(1-\alpha_p)]$ vs pressure based on 21 (●) and 210 μg/mL (■) PIATm. Other conditions were the same as those in Figure 1.

Effects of Pressure and Low Temperature on PIATm. Several studies have described the cold-induced dissociation and denaturation of proteins (*42*−*46*). However, this process is not completely understood. The cold-induced changes in a protein are usually assigned to the disruption of hydrophobic interactions (*42*). Weber (*47*) has proposed that proteins lose stability when subjected to low temperature because of the replacement of the weak bonds of protein−protein interactions by the stronger protein−water interactions. If this is correct, protein folding would reflect an entropy-driven process because of the formation of a great number of weak protein bonds.

Tm has two parallel α helices that produce an extensive contact area essentially supported by weak van der Waals interactions. Because high pressure appears not to lead to complete unfolding of Tm, we repeated the experiment of Figure 2, using a combination of low temperature and high pressure (2.4 kbar), to try to attain complete unfolding. Figure 4 shows the intensity ratio of PIATm subjected to an increase in pressure and a decrease in temperature from +25 to −10 °C. Under 2.4 kbar, low temperature promoted an additional reduction in the fluorescence intensity ratio (I_{485}/I_{385}) of PIATm and a plateau was attained. The final value reached by the combined treatment with high pressure and low temperature is similar to the value obtained by high-temperature denaturation (Figure 5) or urea unfolding (data not shown). This result suggests that pressure and low temperature promote extensive denaturation of Tm. However, it cannot be ascertained from these experiments whether the two chains dissociated.

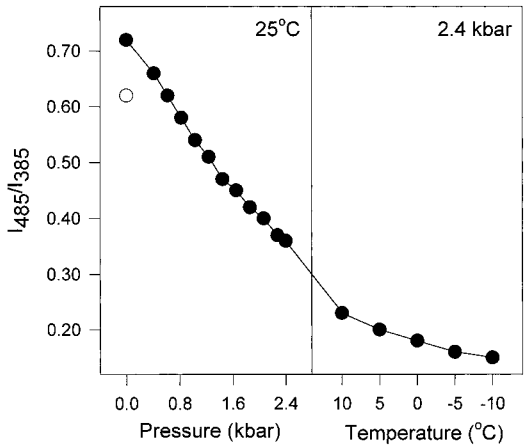

FIGURE 4: Effects of pressure and low temperature on the PIATm fluorescence intensity ratio (I_{485}/I_{385}). PIATm (49 μg/mL) was subjected to 2.4 kbar, and the temperature was decreased to −10 °C (●). The hollow symbol represents the return to initial conditions. Other conditions were the same as those in Figure 1.

PIATm and Tm: High Temperature and Chain Dissociation. To distinguish between the two possible hypotheses to explain the reduced concentration dependence, we used labeled Tm in the presence of unlabeled Tm to verify dissociation. We first characterized the thermal denaturation of Tm. Labeled Tm was subjected to increasing temperatures in the absence and presence of unlabeled Tm (Figure 5). The temperature was raised to 55 °C. Temperatures in the range of 25−40 °C promote an increase in the fluorescence intensity ratio (I_{485}/I_{385}). This phenomenon has been related to a local conformational change of the protein, near Cys 190 (*19*, *34*). It is interesting to note that the initial increase in pyrene excimer fluorescence obtained with temperature was not found with an increase in pressure, probably because the intermediates populated by high temperature and pressure are different.

Higher temperatures caused a progressive decrease in the fluorescence intensity ratio. The value of the intensity ratio reached a plateau at 50 °C for both curves, and the final value was similar to that induced by urea denaturation. After a return to the initial temperature (25 °C), there was an irreversible loss of a significant fraction of the excimer fluorescence when in the presence of a 4-fold excess of unlabeled Tm (Figure 5C). This decrease in the intensity ratio demonstrates that PIATm and Tm were unfolded and dissociated under high temperature, resulting in the exchange of labeled and unlabeled chains when the conditions were returned to room temperature.

It is noteworthy that the excess of unlabeled Tm displaced the temperature curve (Figure 5C) to lower temperatures. Although the unlabeled and labeled proteins unfold at the same temperature, there is a more rapid loss of fluorescence in the presence of unlabeled protein because there is a reversible equilibrium between the two-chain and single-chain species at each temperature. Thus, the reassociated part has fewer pyrene groups to interact with one another. The net effect is a decrease in the T_{50} (temperature that produces 50% of the change) as observed in Figure 5C.

Lack of Subunit Exchange in the Pressure and Cold Denaturation of Tm. PIATm mixed with a 4-fold excess of unlabeled Tm was subjected to 2.4 kbar, and under pressure, the temperature was decreased to −10 °C (Figure 6, filled

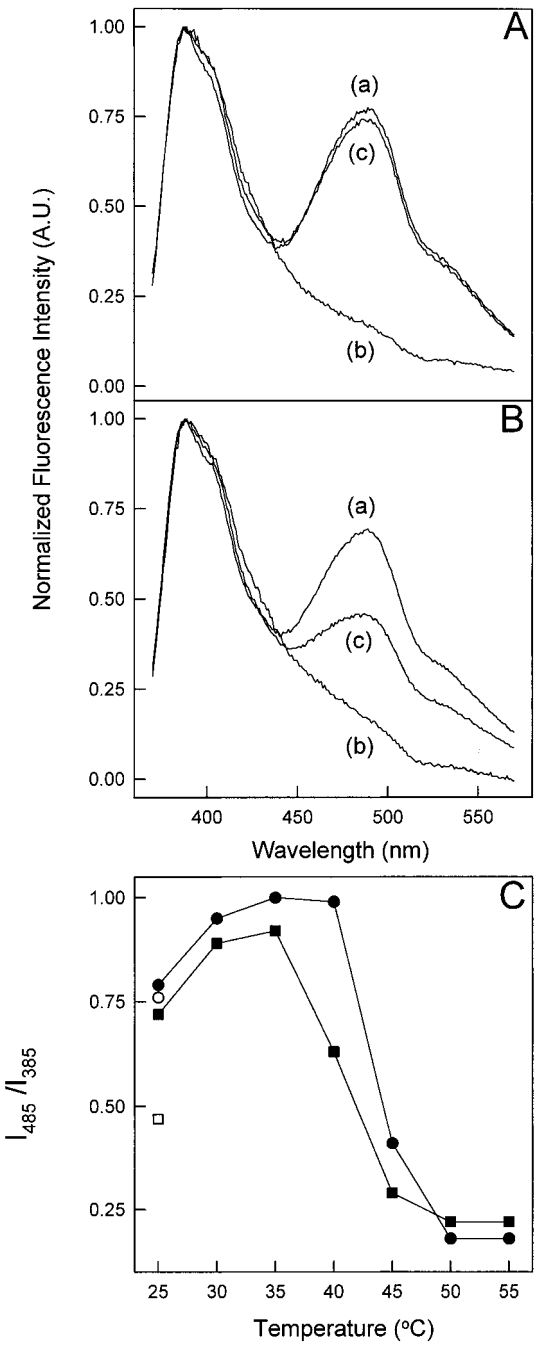

FIGURE 5: Fluorescence emission spectra of PIATm in the absence (A, top) and in the presence (B, middle) of unlabeled Tm. The temperatures were 25 (a), 55 (b), and 25 °C (c). (C, bottom) Effect of temperature on the denaturation of PIATm on the basis of the fluorescence intensity ratio (I_{485}/I_{385}). PIATm in the absence (●) and in the presence (■) of unlabeled Tm. The hollow symbols correspond to the return to 25 °C. The excitation wavelength was 342 nm. Concentrations of PIATm and unlabeled Tm were 49 and 196 μg/mL, respectively. The solvent conditions were the same as those in Figure 1.

square). The fluorescence intensity ratio of PIATm at 2.4 kbar was reduced with a decrease in temperature from +25 to −10 °C. A similar decrease in the intensity ratio of PIATm was observed when the temperature was increased to 55 °C, at atmospheric pressure, in the presence of unlabeled Tm (Figure 5). However, the ratios after returning to the original condition differ markedly in these two experiments. After decompression, the excimer emission returned to the same level observed when only labeled Tm was present. These

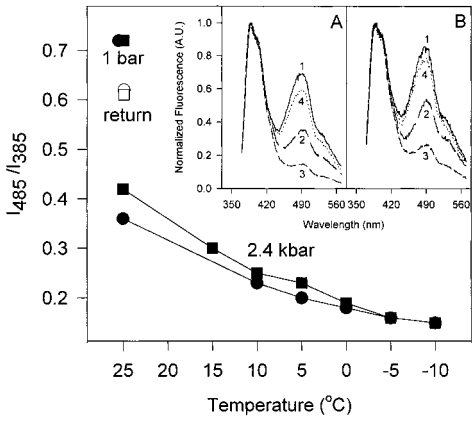

FIGURE 6: Effects of pressure and low temperature on the PIATm fluorescence intensity ratio (I_{485}/I_{385}). PIATm in the absence (●) and in the presence (■) of unlabeled Tm. The hollow symbols correspond to the return to 1 bar and 25 °C. Insets: fluorescence spectra of PIATm in the absence (A) and in the presence (B) of unlabeled Tm. Conditions: at 1 bar and 25 °C (1), at 2.4 kbar and 25 °C (2), at 2.4 kbar and −10 °C (3), and at 1 bar and 25 °C after pressurization and decreasing temperature until −10 °C (4). The excitation wavelength was 342 nm. Concentrations of PIATm and unlabeled Tm were 49 and 196 μg/mL, respectively. Other conditions were the same as those in Figure 1.

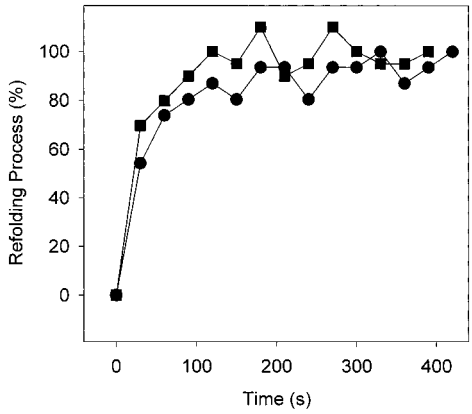

FIGURE 7: Kinetics of refolding. PIATm (1960 μg/mL) was incubated in 8 M urea. At $t = 0$ s, the protein and urea were diluted 40-fold and the refolding process was accompanied by the fluorescence intensity ratio of PIATm (●). PIATm (49 μg/mL) was pressurized to 2.4 kbar (■). After the return to atmospheric pressure at $t = 0$ s, the refolding process was also followed by the fluorescence intensity ratio. Other conditions were the same as those in Figure 1.

results unequivocally demonstrate that the chains were not exchanged under pressure and low temperature because of the preservation of the dimeric structure.

Refolding Kinetics. The results above showed that urea, high temperature, and pressure and low temperature all resulted in a comparable loss of the excimer. Although in all of the cases the states can be named "denatured", the pressure/cold state is mostly dimeric. To determine which steps (dimerization or folding) are limiting the kinetics of formation of the fully folded Tm, refolding experiments were performed at diluted concentrations of protein (Figure 7). Similar time courses were obtained for the refolding of urea-denatured and pressure-denatured Tms upon urea dilution or decompression, respectively.

Changes in Tyrosine Fluorescence and Bis-ANS Binding. Excimer fluorescence is a probe for local and global conformational changes (*48*). To verify whether other

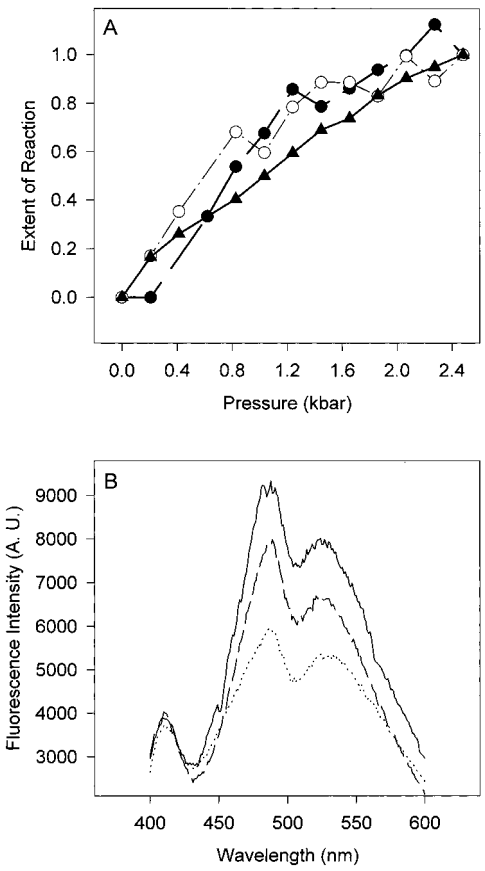

FIGURE 8: Pressure denaturation of Tm as measured by tyrosine and bis-ANS fluorescence. (A) The denaturation of Tm (210 μg/mL) as measured by tyrosine fluorescence center of mass (○), fluorescence of bis-ANS (●), and fraction of pyrene excimer (▲). (B) The fluorescence emission spectra of bis-ANS (210 μg/mL) in the presence of Tm (210 μg/mL), at atmospheric pressure (—) and at 2.4 kbar (− −). The excitation wavelength was 360 nm, and the emission was measured from 400 to 600 nm. The solvent spectrum is represented by a dotted line. Other conditions were the same as those in Figure 1.

changes were occurring in the same pressure range, tyrosine fluorescence and bis-ANS fluorescence were also followed (Figure 8). Tm has 6 tyrosine residues/chain, and changes in its emission are quite representative of global changes in the structure. The Tyr fluorescence emission decreased and underwent a red shift as a function of pressure, indicating substantial denaturation (Figure 8A). Tm bound bis-ANS at atmospheric pressure (Figure 8B) but released the probe when it was completely unfolded by urea. Pressure caused a decrease in bis-ANS fluorescence but not as drastic as that provoked by urea.

The changes produced by pressure in tyrosine and bis-ANS fluorescence were slightly shifted to lower pressures when compared to the decrease in pyrene excimer fluorescence (Figure 8A). This lack of cooperativity among the different spectroscopic probes corroborates the idea that different domains have different susceptibilities to pressure.

DISCUSSION AND CONCLUSIONS

The coiled coil is one of the simplest folding motifs, which is used by many proteins to acquire diverse functions, including gene regulation, viral fusion, and muscle contractility. Here we examined the pressure denaturation of the coiled-coil Tm. Our main finding is that pressure leads to

the formation of a denatured dimer. Low temperature facilitates the pressure denaturation but does not separate the monomers. The formation of a denatured coiled coil reveals an intermediate with folding subdomains, which is likely to be important in the folding pathway of Tm.

In the last years, hydrostatic pressure has been used to provide basic information on the thermodynamics of folding and subunit assembly of many proteins (*22*, *28*). Dimers such as enolase (*32*), β_2 tryptophan synthase (*49*), yeast hexokinase (*50*), Arc repressor (*35*), E2 DNA-binding protein (*51*, *52*), and LexA repressor (*37*) showed the same typical behavior: concentration dependence of the dissociation process. The dissociation curves of these dimers were displaced to higher pressures when the protein concentration increased, and the $\Delta p_{1/2}$ obtained experimentally was in good agreement with that calculated from eq 4.

More recently, the dissociation of a dimer occurred with no concentration dependence, which the authors attributed to subunit heterogeneity (*53*). The denaturation of the associated fragments of chymotrypsin inhibitor 2 also occurred without concentration dependence, but in this case, the complex (both fragments) was demonstrated to denature without dissociation first (*54*). In a similar way, Arc repressor also denatured as a dimer by high temperature at high protein concentrations (*55*). More recently, the pressure-induced population of an amyloidogenic state of transthyretin was not very dependent on protein concentration (*56*). Smaller changes in the protein conformation preceding dissociation have also been reported for dimers (*57*, *58*) and viruses (*29*).

Large multisubunit complexes such as erythrocruorin (*39*), hemocyanin (*41*), protein aggregates (*59*), and tetramers subjected to low temperatures (*40*) showed independence of pressure effects upon the concentration. Because in those cases dissociation indeed occurred, the nonstochastic behavior was explained by a physical heterogeneity, in which each particle responds to pressure independently of the others.

In the case of Tm, the $p_{1/2}$ increased only 200 bar when the protein concentration changed 10-fold. This value was 33% of that expected for the dynamic equilibrium of a monomer $\leftrightarrow$ dimer system with a volume change of association of 57 mL/mol and $C_2/C_1 = 10$. The exchange experiments for thermal (Figure 5) and pressure/cold (Figure 6) denaturation demonstrated unambiguously that the two physical means to perturb the Tm structure lead to different species. High temperature results in unfolded monomers of Tm, whereas high pressure and low temperature induce a denatured dimer of Tm. The decrease of the concentration dependence of PIATm indicates that pressure produces subdomain denaturation and the polypeptide chains do not separate. The small concentration dependence may be the result of partly unfolded chains of different dimers interacting with one another. This hypothesis is in agreement with the results obtained by Ishii et al. (*12*). They showed by far-UV circular dichroism a lesser degree of stability for the central region of the structure surrounding Cys 190. Noncooperative denaturation is also suggested by the tyrosine and bis-ANS fluorescence data (Figure 8).

Previous studies with high pressure indicated that the dissociation of oligomeric proteins is facilitated by low temperatures (*36*, *43*, *44*, *47*, *49*). Here, we find that high pressure associated to low temperature did not promote the complete dissociation of PIATm. As is shown in Figure 6, subzero temperature induced an additional reduction in the fluorescence intensity ratio (I_{485}/I_{385}), similar to that obtained by high temperature (55 °C) and urea (not shown). However, the labeled and unlabeled chains were not exchanged, as would be expected for the full dissociation of the protein. We suggest that the conformational change induced by pressure and low temperature is more limited than that promoted by high temperature (55 °C). Our pressure data agree with a previous proposal based on calorimetric data (*60*) that assigns the melting of a coiled-coil structure to several discrete stages corresponding to the disruption of distinct cooperative blocks of the molecule. Then, the intermediate state isolated by pressure and low temperature probably has unfolded and partially folded parts, simultaneously. The unfolded part probably corresponds to the more unstable sites in the structure. The volume change of the subdomain unfolding for the PIATm is −34 mL/mol. This volume change probably reflects the average change in volume between the knots, as is represented schematically in Figure 9. This volume change is similar to the value obtained for the dissociation of the coiled-coil dimer of the leucine zipper GCN4-p1 (Silva et al., unpublished results). In the case of this leucine zipper, dissociation occurs because it is a short coiled coil (33 amino acid residues/polypeptide).

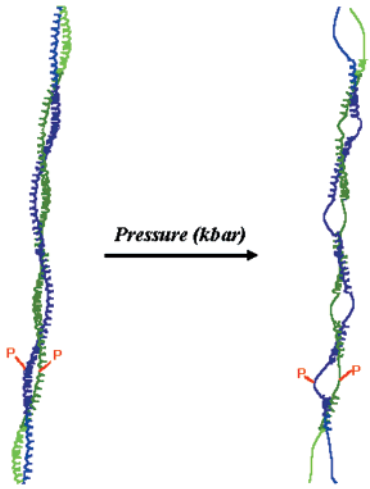

FIGURE 9: Proposed conformational change of PIATm induced by 2.4 kbar. Segments which lack secondary structure are linked by knots, which keep the chains together.

Overall, our data indicate that pressure or pressure and low temperature causes a large structural change in Tm. The combined effects of pressure and low temperature result in the same level of excimer as those produced by high temperature or high concentrations of urea. However, the absence of exchange (Figure 6) and the reduced concentration dependence indicate that most of the pressure-denatured species are dimeric. The lack of exchange between labeled and unlabeled Tm also indicates a subdomain denaturation. The model depicted in Figure 9 shows a transition between native dimeric Tm and subdomain denatured Tm, where segments that lack secondary structure are linked by knots which keep the chains together. Our data do not allow us to determine the location and number of these knots. However, the relatively small volume change of 34 mL/mol correlates to a molecular volume of about 57 Å^3, which corresponds to a calculated value of exposure of a buried area of 1244 Å^2, assuming the linear compressibility of a nonpolar solvent

(*61*). Accordingly, noncooperative units with this average exposed surface area would break, generating a structure as depicted in Figure 9. Our model is also in accordance with a recent theoretical explanation for pressure effects on proteins (*62*), where pressure causes the molecules of water to infiltrate into the hydrophobic core of the protein. In the case of a coiled coil such as Tm, our results clearly show that there are soft (pressure-sensitive knots) and hard (pressure-insensitive knots) sites. Therefore, packing seems to be crucial in determining the folding of Tm, and the state we isolate under pressure and low temperature is likely a kinetic intermediate formed during the folding of Tm. The experiment in Figure 7 shows that the rate of refolding from the urea-denatured monomers is similar to that observed on refolding from the pressure-denatured dimer. Although the deadtime for the pressure experiment did not permit us to explore times below 15 s, our results indicate that the isomerization is the limiting step. These results agreed with a detailed kinetic study of the self-assembly of αα-Tm from rabbit cardiac muscle, which revealed a slow first-order phase (*63*).

In the 1970s, there was the hierarchical concept that the assembly of oligomeric proteins follows a single route for the formation of the different structural levels: (1) independent units of secondary structure and domains → (2) fully folded monomer → (3) association into oligomers. However, in the last 20 years, the folding of proteins has revealed a much higher plasticity and multiplicity of routes. There are examples including folding from practically unfolded monomers (*64*), formation of immature oligomers (*65*, *66*) that isomerize to the biologically active forms, and transient aggregation in the pathway of folding (*67*). In the case of a long coiled coil, such as Tm, the fast formation of a structure similar to the one depicted in Figure 9 may prevent multiple coiling and aggregation. The model of Figure 9 shows what can be a general scheme for long two-stranded coiled coils: The isomerization from the "knotted structure" to the functional form is the rate-limiting step. According to this model, it is relatively immaterial how long the structure is, which facilitates a lot the folding and assembly of coiled coils.

ACKNOWLEDGMENT

We thank Martha Sorenson for the critical reading of the manuscript and suggestions and Emerson Gonçalves for his competent technical assistance.

REFERENCES

1. Lupas, A. (1996) *Trends Biochem. Sci. 21*, 375−382.
2. O'Shea, E. K., Rutkowski, R., and Kim, P. S. (1989) *Science 243*, 538−542.
3. Lehrer, S. S., Qian, Y. D., and Hvidit, S. (1989) *Science 246*, 926−928.
4. Hatzfeld, M., and Weber, K. (1990) *J. Cell Biol. 110*, 1199−1210.
5. Skehel, J. J., and Wiley, D. C. (1998) *Cell 95*, 871−874.
6. Chan, C., and Kim, P. S. (1998) *Cell 93*, 681−684.
7. Harbury, P. B., Zhang, T., Kim, P. S., and Alber, T. (1993) *Science 262*, 1401−1407.
8. Lumb, K. J., Carr, C. M., and Kim, P. S. (1994) *Biochemistry 33*, 7361−7367.
9. Oakley, M. G., and Kim, P. S. (1998) *Biochemistry 37*, 12603−12610.
10. Bhattacharyya, R. P., and Sosnick, T. R. (1999) *Biochemistry 38*, 2601−2609.
11. Lehrer, S. S. (1978) *J. Mol. Biol. 118*, 209−226.
12. Ishii, Y., Hitchcock-Degregori, S., Mabuchi, K., and Lehrer, S. S. (1992) *Protein Sci. 1*, 1319−1325.
13. Greenfield, N. J., and Hitchcock-DeGregori, S. E. (1993) *Protein Sci. 2*, 1263−1273.
14. Holtzer, M. E., and Holtzer, A. (1992) *Biopolymers 32*, 1589−1591.
15. Lehrer, S. S., and Yuan, A. (1998) *J. Struct. Biol. 122*, 176−179.
16. Johnson, P., and Smillie, L. B. (1975) *Biochem. Biophys. Res. Commun. 64*, 1316−1322.
17. Stone, D., and Smillie, L. B. (1978) *J. Biol. Chem. 253*, 1137−1148.
18. Flicker, P. F., Phillips, G. N., Jr., and Cohen, C. (1982) *J. Mol. Biol. 162*, 495−501.
19. Ishii, Y., and Lehrer, S. S. (1990) *Biochemistry 29*, 1160−1166.
20. Silva, J. L., and Weber, G. (1993) *Annu. Rev. Phys. Chem. 44*, 89−113.
21. Jonas, J., and Jonas, A. (1994) *Annu. Rev. Biophys. Biomol. Struct. 23*, 287−318.
22. Heremans, K., and Smeller, L. (1998) *Biochim. Biophys. Acta 1386*, 353−370.
23. Panick, G., Vidugiris, G. J., Malessa, R., Rapp, G., Winter, R., and Royer, C. A. (1999) *Biochemistry 38*, 4157−4164.
24. Torrent, J., Connelly, J. P., Coll, M. G., Ribo, M., Lange, R., and Vilanova, M. (1999) *Biochemistry 48*, 15952−15961.
25. Hillson, N., Onuchic, J. N., Garcia, A. E. (1999) *Proc. Natl. Acad. Sci. U.S.A. 96*, 14848−14853.
26. Prevelige, P., King, J., and Silva, J. L. (1994) *Biophys. J. 66*, 1631−1641.
27. Gorovits, B., Raman, C. S., Horowitz, P. M. (1995) *J. Biol. Chem. 270*, 2061−2066.
28. Silva, J. L., Foguel, D., Da Poian, A. T., and Prevelige, P. E. (1996) *Curr. Opin. Struct. Biol. 6*, 166−175.
29. Leimkuhler, M., Goldbeck, A., Lechner, M. D., and Witz, J. (2000) *J. Mol. Biol. 296*, 1295−1305.
30. Oliveira, A. C., Gomes, A. M. O., Almeida, F. C. L., Mohana-Borges, R., Valente, A. P., Reddy, V. S., Johnson, J. E., and Silva, J. L. (2000) *J. Biol. Chem. 275*, 16037−16043.
31. Neuman, R. C., Kauzmann, W., and Zipp, A. (1973) *J. Phys. Chem. 77*, 2687−2691.
32. Paladini, A. A., and Weber, G. (1981) *Biochemistry 20*, 2587−2593.
33. Betcher-Lange, S., and Lehrer, S. S. (1978) *J. Biol. Chem. 253*, 3757−3760.
34. Graceffa, P., and Lehrer, S. S. (1980) *J. Biol. Chem. 23*, 11296−11300.
35. Silva, J. L., Silveira, C. F., Correia, A., Jr., and Pontes, L. (1992) *J. Mol. Biol. 223*, 545−555.
36. Erijman, L., Lorimer, G. H., and Weber, G. (1993) *Biochemistry 32*, 5187−95.
37. Mohana-Borges, R., Pacheco, A. B. F., Sousa, F. J. R., Foguel, D., Almeida, D. F., and Silva, J. L. (2000) *J. Biol. Chem. 275*, 4708−4712.
38. Da Poian, A. T., Oliveira, A. C., Gaspar, L. P., Silva, J. L., and Weber, G. (1993) *J. Mol. Biol. 231*, 999−1008.
39. Silva, J. L., Villas-Boas, M., Bonafe, C. F. S., and Meireles, N. C. (1989) *J. Biol. Chem. 264*, 15863−15868.
40. Erijman, L., and Weber, G. (1991) *Biochemistry 30*, 1595−1599.
41. Bonafe, C. F. S., Araujo, J. R., and Silva, J. L. (1994) *Biochemistry 33*, 2651−2660.
42. Privalov, P. L. (1990) *Crit. Rev. Biochem. Mol. Biol. 4*, 281−305.
43. Foguel, D., Chaloub, R. M., Silva, J. L., Crofts, A. R., and Weber, G. (1992) *Biophys. J. 63*, 1613−1622.
44. Foguel, D., and Silva, J. L. (1994) *Proc. Natl. Acad. Sci. U.S.A. 91*, 8244−8247.
45. Foguel, D., and Weber, G. (1995) *J. Biol. Chem. 48*, 28759−28766.

46. Nash, D. P., and Jonas, J. (1997) *Biochemistry 36*, 14375−14383.
47. Weber, G. (1993) *J. Phys. Chem. 97*, 7108−7115.
48. Ishii, Y. (1994) *Eur. J. Biochem. 221*, 705−12.
49. Silva, J. L., Miles, E. W., and Weber, G. (1986) *Biochemistry 25*, 5780−5786.
50. Ruan, K., and Weber, G. (1988) *Biochemistry 27*, 3295−3301.
51. Foguel, D., Silva, J. L., and Prat-Gay, G. (1998) *J. Biol. Chem. 273*, 9050−9057.
52. Lima, L. M. T. R., Foguel, D., and Silva, J. L. (2000) *Proc. Natl. Acad. Sci. U.S.A. 97*, 14289−14294.
53. Rietveld, A. W. M., and Ferreira, S. T. (1996) *Biochemistry 35*, 7743−7751.
54. Mohana-Borges, R., Silva, J. L., and Prat-Gay, G. (1999) *J. Biol. Chem. 274*, 7732−7740.
55. Robinson, C., Rentzeperis, D., Silva, J. L., and Sauer, R. T. (1997) *J. Mol. Biol. 273*, 692−700.
56. Ferrão-Gonzales, A. D., Souto, S. O., Silva, J. L., Foguel, D. (2000) *Proc. Natl. Acad. Sci. U.S.A. 97*, 6445−6450.
57. Peng, X., Jonas, J., and Silva, J. L. (1994) *Biochemistry 33*, 8323−8329.
58. Zhou, J. M., Zhu, L., and Balny, C. (2000) *Eur. J. Biochem. 267*, 1247−1253.
59. St John, R. J., Carpenter, J. F., and Randolph, T. W. (1999) *Proc. Natl. Acad. Sci. U.S.A. 96*, 13029−13033.
60. Potekhin, S. A., and Privalov, P. L. (1982) *J. Mol. Biol. 159*, 519−535.
61. Foguel, D., Suarez, M. C., Barbosa, C., Rodrigues, J. J., Sorenson, M. M., Smillie, L. B., and Silva, J. L. (1996) *Proc. Natl. Acad. Sci. U.S.A. 93*, 10642−10646.
62. Hummer, G., Garde, S., Garcia, A. E., Paulaitis, M. E., and Pratt, L. R. (1998) *Proc. Natl. Acad. Sci. U.S.A. 95*, 1552−1555.
63. Mo, J. M., Holtzer, M. E., and Holtzer, A. (1991) *Proc. Natl. Acad. Sci. U.S.A. 88*, 916−920.
64. Milla, M. E., Brown, B. M., Waldburger, C. E., and Sauer, R. T. (1995) *Biochemistry 34*, 13914−13919.
65. Goldenberg, D., and King, J. (1982) *Proc. Natl. Acad. Sci. U.S.A. 79*, 3403−3407.
66. Blond, S., and Goldberg, M. E. (1985) *J. Mol. Biol. 182*, 597−606.
67. Silow, M., Yee-Joo, T., Fersht, A. R., and Oliveberg, M. (1999) *Biochemistry 38*, 13006−13012.

BI0020978